Electronic Supplementary Information for

Insights into the Behavior of Nonanoic Acid and Its Conjugate Base at the Air/Water Interface Through a Combined Experimental and Theoretical Approach

Man Luo[1], Nicholas A. Wauer[1], Kyle J. Angle[1], Abigail C. Dommer[1], Meishi Song[1], Christopher M. Nowak[1], Rommie E. Amaro[1*], Vicki H. Grassian[1,2*]

[1]Department of Chemistry and Biochemistry, University of California, San Diego, La Jolla, CA 92093

[2]Department of Nanoengineering and Scripps Institution of Oceanography, University of California, San Diego, La Jolla, CA 92093

Table of Contents

*Authors to whom correspondence should be addressed

Derivations & Equations

$$\delta_{obs} = f_{HA}\delta_{HA} + f_{A^-}\delta_{A^-} \quad \text{eq. S1}$$

f, mole fraction; and δ, chemical shift of protonated and deprotonated nonanoic acid

$$f_{HA} = \frac{[H^+]}{[H^+]+K_a} \quad \text{eq. S2}$$

$$f_{A^-} = \frac{K_{A^-}}{[H^+]+K_a} \quad \text{eq. S3}$$

K_a is the acid dissociation constant and $[H^+]$ is the concentration of hydronium ion in the solution.

Modified model calculation from Badban et al., for the surface adsorption of deprotonated nonanoic acid[1]:

From thermodynamics:

$$d\gamma = -RT\sum_i \Gamma_i \, d(\ln(c_i)) \quad \text{eq. S4}$$

Define: $$K_A = \frac{\Gamma_{A^-}}{\Gamma_v c_{A^-}} \quad \text{eq. S5}$$

$$K_{HA} = \frac{\Gamma_{HA}}{\Gamma_v c_{HA}} \quad \text{eq. S6}$$

Define: $\Gamma_{max} = \Gamma_v + \Gamma_{A^-} + \Gamma_{HA}$ (assume Na^+ does not occupy any surface sites) eq. S7

Use eq. S5 & S6 & S7 to derive:

$$\Gamma_v = \frac{\Gamma_{max}}{1+K_{A^-}c_{A^-}+K_{HA}c_{HA}} \quad \text{eq. S8}$$

Use eq. S5 & S8 to derive:

$$\Gamma_A = \Gamma_{max}\frac{K_{A^-}c_{A^-}}{1+K_{A^-}c_{A^-}+K_{HA}c_{HA}} \quad \text{eq. S9}$$

Use eq. S6 and S8 to derive:

$$\Gamma_{HA} = \Gamma_{max}\frac{K_{HA}c_{HA}}{1+K_{A^-}c_{A^-}+K_{HA}c_{HA}} \quad \text{eq. S10}$$

For nonanoic acid solutions at pH 11-12 with a constant concentration of Na^+:

$$d\gamma = -RT(\Gamma_{A^-} d\ln(c_{A^-}) + \Gamma_{HA} d\ln(c_{HA}) + \Gamma_{OH^-} d\ln(c_{OH^-}) + \Gamma_{Na^+} d\ln(c_{Na^+}))$$

$$= -RT(\Gamma_{A} d\ln(c_{A^-}) + \Gamma_{HA} d\ln(c_{HA}) + \Gamma_{OH^-} d\ln(c_{OH^-}) \quad \text{eq. S11}$$

Naturally we have: $k_a = \frac{c_{A^-}}{c_{HA}} c_{H_3O^+} = \frac{c_{A^-}}{c_{HA}} \frac{k_w}{c_{OH^-}}$ eq. S12

Therefore, we have: $d\ln(c_{OH^-}) = d\ln(c_{A^-}) - d\ln(c_{HA})$ eq. S13

Eq. 11 is simplified as:

$$d\gamma = -RT((\Gamma_{A^-} + \Gamma_{OH^-}) d\ln(c_{A^-}) + (\Gamma_{HA} - \Gamma_{OH^-}) d\ln(c_{HA})) \quad \text{eq. S14}$$

At a constant NaOH of 20 mM, we have:

$$k_a = \frac{c_A [H^+]}{c_{HA}} = \frac{c_{A^-} k_w}{(c_{total} - c_{A^-})[OH^-]} \quad \text{eq. S15}$$

$$c_{A^-} + [OH^-] = 0.02 \quad \text{eq. S16}$$

Rearrange eq. S15 and substitute it into eq. S16, we get:

$$c_{A^-} + \frac{c_{A^-} k_w}{(c_{total} - [c_{A^-}]) k_a} = 0.02 \quad \text{eq. S17}$$

Rearrange eq. S17 to get:

$$c_{A^-}{}^2 - (0.02 + c_{total} + \frac{k_w}{k_a})\, c_{A^-} + 0.02\, c_{total} = 0 \quad \text{eq. S18}$$

Therefore, we obtain

$$c_{A^-} = \frac{\left(0.02 + c_{total} + \frac{k_w}{k_a}\right) - \sqrt{(0.02 + c_{total} + \frac{k_w}{k_a})^2 - 4 * 0.02 c_{total}}}{2} \quad \text{eq. S19}$$

Then $\ln(c_{A^-})$ was calculated at different c_{total} and plotted against $\ln(c_{total})$. c_{HA} was calculated by (c_{total} - c_{A^-}), and $\ln(c_{HA})$ was plotted against $\ln(c_{total})$ as well. The plot can be seen in Figure S9. Therefore, we obtain:

$$d\ln(c_{HA}) = 1.02 * d\ln(c_{A^-}), \quad (10^{-8}\ \text{M} < c_{A^-} < 10^{-2}\ \text{M}) \quad \text{eq. S20}$$

Therefore, we obtain:

$$-\frac{1}{RT}\frac{d\gamma}{d(lnc_{A^-})} = \Gamma_{A^-} + 1.02\Gamma_{HA} - 0.02\Gamma_{OH^-}$$

$$= \Gamma_{max}\left(\frac{K_{A^-}c_{A^-}+1.02K_{HA}c_{HA}}{1+K_{A^-}c_{A^-}+K_{HA}c_{HA}}\right) - 0.02\Gamma_{OH^-} \quad \text{eq. S21}$$

Since at basic pH around 11, $c_{HA} << c_{A^-}$, therefore we simplified eq. S21 to:

$$-\frac{1}{RT}\frac{d\gamma}{d(lnc_{A^-})} = \Gamma_{max}\left(\frac{K_{A^-}c_{A^-}}{1+K_{A^-}c_{A^-}}\right) - 0.02\Gamma_{OH^-} \quad \text{eq. S22}$$

After we fit eq. S22 with experimental data, we found the best fit for the term Γ_{OH} is 0, therefore eq. S22 become eq. S23 below:

$$-\frac{1}{RT}\frac{d\gamma}{d(lnc_{A^-})} = \Gamma_{max}\left(\frac{K_{A^-}c_{A^-}}{1+K_{A^-}c_{A^-}}\right) \quad \text{eq. S23}$$

γ: surface tension (mN/m)

R: ideal gas constant

T: temperature (K)

c_i (i = A^-, HA, OH^-, total): bulk concentration of nonanoate (A^-), neutral nonanoic acid (HA), hydroxide ion (OH^-), and total bulk concentration of nonanoic acid (total) (M)

Γ_i(i = A^-, HA, OH^-): surface excess concentration (mol/m^2)

K_{A^-} & K_{HA}: adsorption constant (M^{-1})

Γ_v: vacant surface excess (mol/m^2)

Γ_{max}: total available surface excess on the surface (mol/m^2)

k_a: acid association constant (M)

k_w: autoionization constant for water (M)

Figures

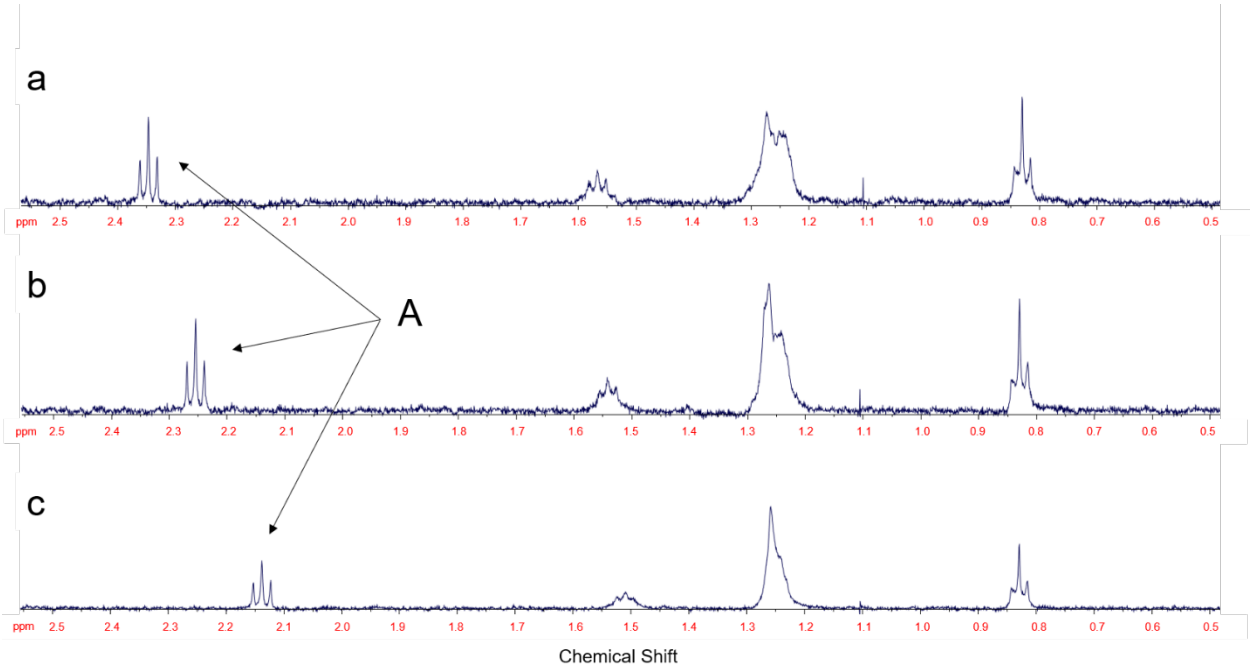

Figure S1. NMR spectra for 0.9 mM nonanoic acid in pH 3 (a), pH 5 (b), and pH 9 (c) solutions. Peak A represents the hydrogens on the carbon next to the carboxylic/carboxylate group on nonanoic acid. The chemical shift of peak A is used to determine the protonation state of nonanoic acid as the observed chemical shift can be expressed as a weighted average of chemical shifts from protonated and deprotonated species and the weighing factors are their mole fraction,[2] which can be expressed as eq. S1.

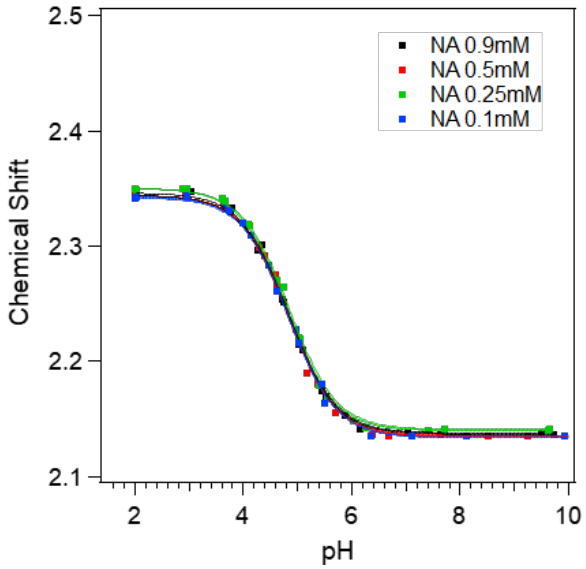

Figure S2. Chemical shift of peak A vs. pH plot from NMR spectra at different nonanoic acid concentrations. Based on eq. S1 and the description of the mole fraction from eq. S2 and S3, we can obtain the bulk pK_a for nonanoic acid at different concentration by fitting the experimental data.[2] The dots represent the experimental data and the lines are fitted curves. No obvious difference of bulk pK_a was found between different nonanoic acid concentrations, which is 4.8 ± 0.1.

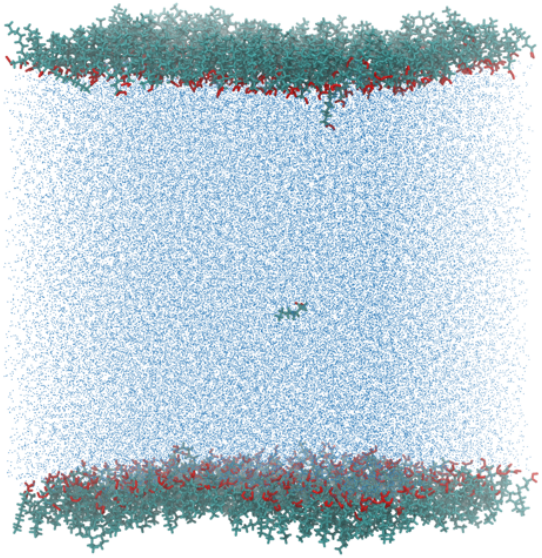

Figure S3. The system for the monolayer alchemical FEP calculations had two 100 Å x 100 Å nonanoic acid leaflets (hydrocarbon tails in cyan, carboxylic acids in red) separated by a 100 Å x 100 Å x 100 Å water box (blue dots) with a single nonanoic acid in bulk solution. The FEP/MD system for a single nonanoic acid at the surface was set up the same way but replaced the two leaflets with a lone acid at each air/water interface.

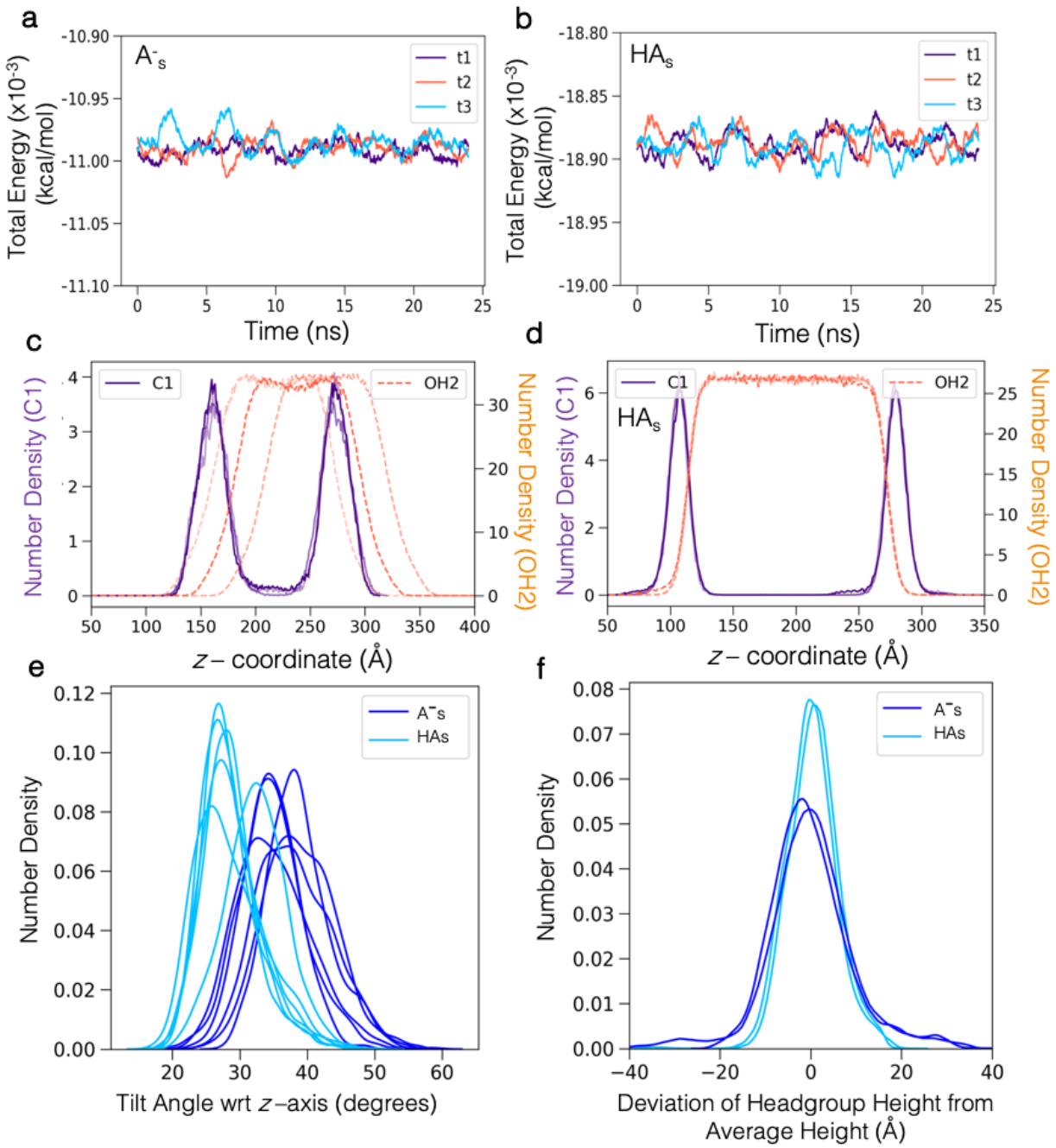

Figure S4: Markers of protonated vs deprotonated nonanoic acid monolayer stability. a-b) Plots of the total energy for the deprotonated (a) and protonated (b) systems over the duration of each production simulation. The total energy remains stable over the 25-ns, indicating the systems have approached equilibrium. c-d) Z-distribution of the nonanoic acid headgroups (purple) and the water molecules (orange) for deprotonated (c) and protonated (d) nonanoic acid. The broad distribution of nonanoic acid headgroups in (c) indicate that the monolayer has deformed from its planar organization to allow for increased coordination with sodium cations. Additionally, the plots show that the water density on one side of the system has shifted outside of the headgroups, indicating partial dissolution of the monolayer in the timescale of the simulation. In comparision, the sharp, narrow peaks in (d) are indicative of headgroups aligned well with the interfacial plane; thus, the protonated form adopts a more stable monolayer. The condensed headgroups of (c) relative to (d) indicate the compression of the system to allow for greater ion-complexation; this behavior has been

noted before.[3] Plot (e) is a representation of the distribution of molecular tilt angles with respect to the perpendicular z-axis. The tilt angles were calculated by analyzing the vector formed by the C1-C9 pair and computed as the angle between that and the vector normal. A narrow distribution of tilt angles shown by HA (light blue) suggests the alignment of the lipids to one another in a raft formation; the broad distribution given by A- suggests the opposite: the monolayer has become disrupted and the lipids no longer align. Finally, plot (f) shows the distribution of headgroup deviations from the monolayer average height. This is consistent with plots (c-d) in that there is a broader distribution of headgroups in the deprotonated monolayer relative to the protonated. Taken together, these plots are indicative of MD system health and corroborate the evidence supplied in this work that nonanoic acid is less acidic at the surface, despite any weakly-stabilizing salt effects.

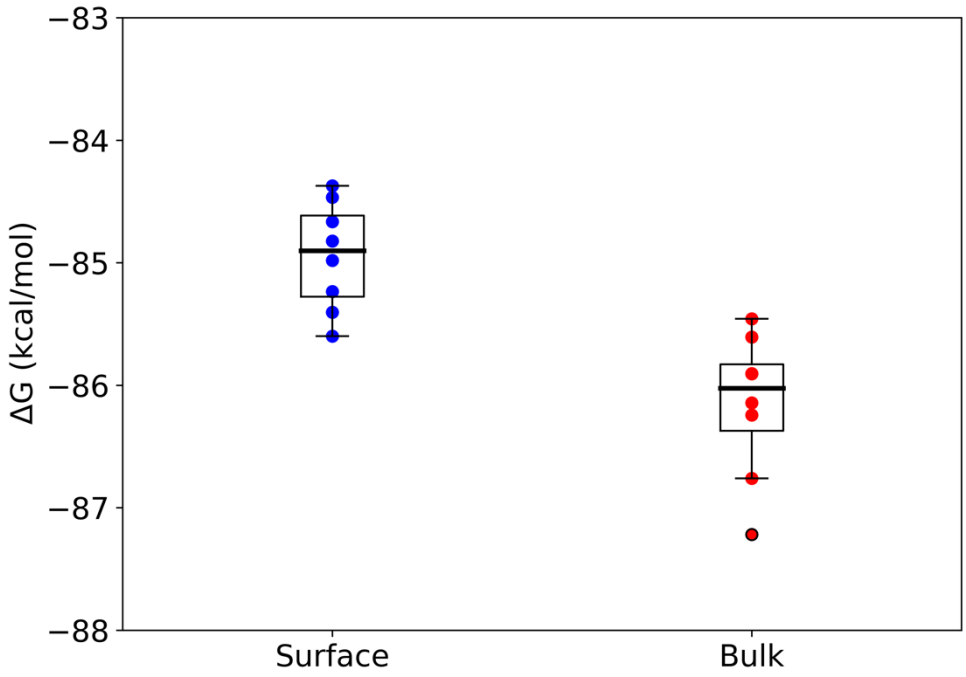

Figure S5. Box and whisker plots of the free energy change of deprotonation calculated for each microenvironment in the FEP/MD simulations for the system with a single nonanoic acid at the surface (n=8). Mean ± stdev: $\Delta G_{deprot}^{surface} = -84.9 \pm 0.4$ kcal/mol and $\Delta G_{deprot}^{bulk} = -86.2 \pm 0.6$ kcal/mol

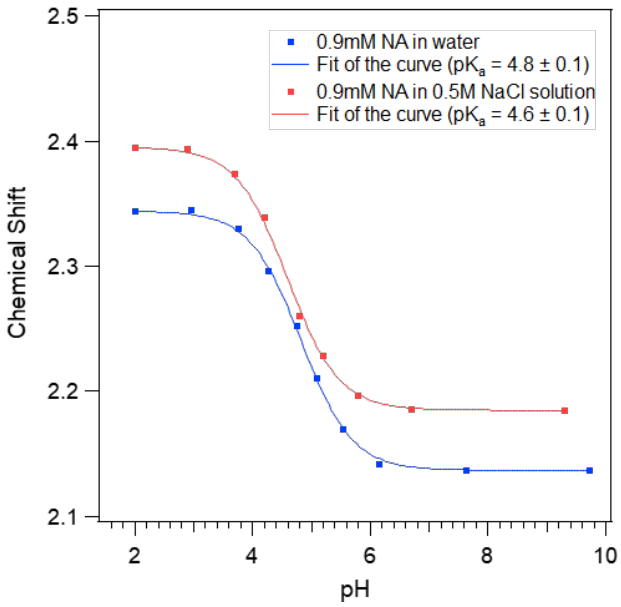

Figure S6. Chemical shift of peak A vs. pH plot from NMR spectra for nonanoic acid in water compared with in 0.5 M NaCl solution. The bulk pK_a is calculated from eq. S1, S2 and S3.

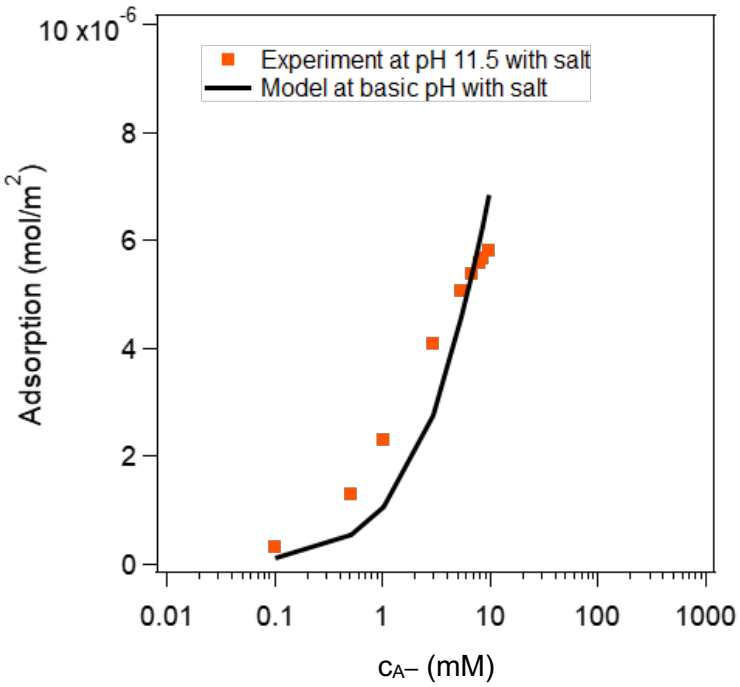

Figure S7. Model fitting for nonanoic acid surface adsorption at pH 11.5 ± 0.5 with a constant concentration of NaOH (20 mM) and a constant concentration of NaCl (0.5 M). The orange dots represent the left-hand side of eq. S23 (eq. 6 in the main text) from the experimental data and the black line represent the right-hand side of eq. S23 (eq. 6 in the main text) with best fit of the parameters.

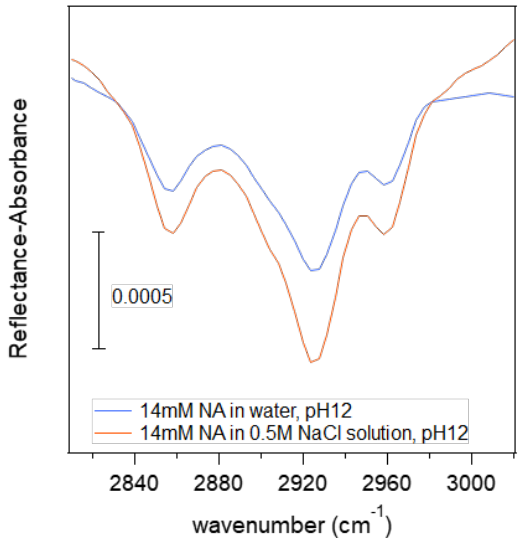

Figure S8. IRRAS spectra for 14 mM nonanoic acid in water compared to in 0.5 M NaCl solution at pH 12.

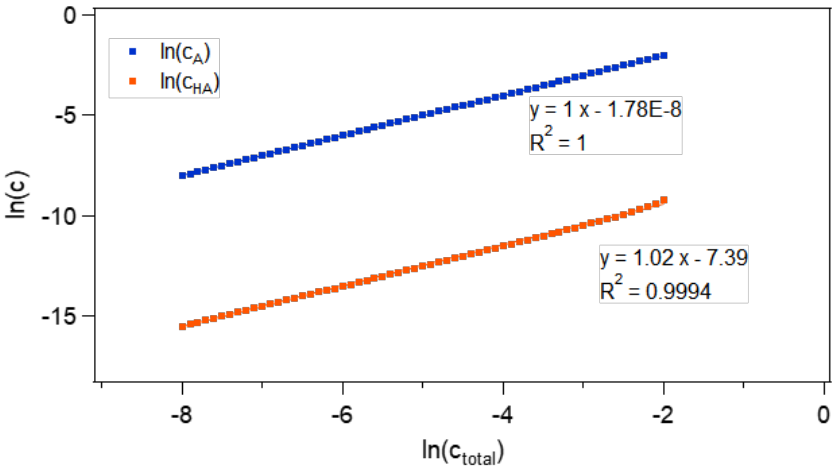

Figure S9. Correlations between c_A and c_{HA} versus total nonanoic acid concentration under constant NaOH (20 mM) condition.

References:

1 S. Badban, A. E. Hyde and C. M. Phan, *ACS Omega*, 2017, **2**, 5565–5573.

2 A. Lopalco, J. Douglas, N. Denora and V. J. Stella, *J. Pharm. Sci.*, 2016, **105**, 664–672.

3 E. M. Adams, B. A. Wellen, R. Thiraux, S. K. Reddy, A. S. Vidalis, F. Paesani and H. C. Allen, *Phys. Chem. Chem. Phys.*, 2017, **19**, 10481–10490.